Available online at www.sciencedirect.com
SCIENCE DIRECT®
International Journal of Mass Spectrometry 230 (2003) 193–200
International Journal of Mass Spectrometry
www.elsevier.com/locate/ijms

Gas-phase dissociation pathways of a tetrameric protein complex

Frank Sobott, Margaret G. McCammon, Carol V. Robinson*

Chemistry Department, Cambridge University, Lensfield Road, Cambridge CB2 1EW, UK

Received 31 August 2003; accepted 8 September 2003

This paper is dedicated to Professor J.H. Beynon, FRS, on his 80th birthday. John inspired those around him. Through him I learnt the importance of commitment to science as well as a fascination for metastable ions

Abstract

The gas-phase dissociation of the tetrameric complex transthyretin (TTR) has been investigated with tandem-mass spectrometry (tandem-MS) using a nanoflow-electrospray interface and a quadrupole time-of-flight (Q-TOF) mass spectrometer. The results show that highly charged monomeric product ions dissociate from the macromolecular complex to form trimeric products. Manipulating the pressure conditions within the mass spectrometer facilitates the formation of metastable ions. These were observed for the transitions from tetrameric to monomeric and trimeric product ions and additionally for losses of small molecules associated with the protein complex in the gas phase. These results are interpreted in the light of recent mechanisms for the electrospray process and provide insight into the composition and factors governing the stability of macromolecular ions in the gas phase.

Keywords: Protein complex; Noncovalent interaction; Collision-induced dissociation; Metastable decomposition

1. Introduction

The plethora of multiprotein complexes that have been preserved in the gas phase and recorded by mass spectrometry (MS) in recent years prompt research into understanding their gas-phase structure and composition [1–3]. While it is widely accepted that the mass spectra of protein complexes under the appropriate conditions can be used to determine the stoichiometry of interacting subunits, relatively few reports describe the application of tandem-MS approaches to examine macromolecular complexes. Examples that have been reported include the isolation and collision-induced dissociation (CID) of a tetramer of streptavidin using Fourier transform-ion cyclotron resonance (FT-ICR) MS, where an asymmetric distribution of charge between the monomeric and trimeric product ions was observed [4]. More recently, investigations of homodimers reveal unequal distributions of charge in the resulting monomers [5], as well as metastable ions formed via slow decay of the collisionally activated dimer in the reflectron-time-of-flight (TOF) mass analyser [6]. We have demonstrated the use of gas-phase dissociation of hetero-oligomeric assemblies, specifically in a hexameric molecular chaperone complex [7] and in the heterogeneous complex formed between transthyretin (TTR), thyroxin, retinol-binding protein and retinol [8]. While it is tempting to suggest that subunits of the periphery of the complex dissociate more readily than those in the core at the present time, it is not clear if this will always be the case. It is anticipated that a greater understanding of the dissociation pathways of multiprotein complexes in the gas phase will extend the ability of the technique to be applied to examine complexes of unknown composition and structure. In addition, the metastable decay of species which originate from a selected charge state of the protein complex can give valuable insight into the composition of the multiprotein complex.

The composition of macromolecular complex ions in the gas phase requires an understanding of their formation from solution. Recent reports have suggested that there is general consensus about the initial events of the electrospray process at least for globular proteins from aqueous solution in ammonium acetate buffers [9]. In the electrospray process, the bulk solution is dispersed into a stream of droplets

Abbreviations: CID, collision-induced dissociation; ESI, electrospray ionisation; FT-ICR, Fourier transform-ion cyclotron resonance; MS, Mass spectrometry/mass spectrometer; Nano-ESI, nanoflow-electrospray ionisation; Q-TOF, quadrupole time-of-flight; TTR, transthyretin

* Corresponding author. Tel.: +44-1223-763846; fax: +44-1223-763843.
E-mail address: cvr24@cam.ac.uk (C.V. Robinson).

1387-3806/$ – see front matter © 2003 Elsevier B.V. All rights reserved.
doi:10.1016/j.ijms.2003.09.008

[10]. The 'Rayleigh fission' model predicts that coulombic repulsion between like charges in the shrinking droplet leads to asymmetric dissociation when the repulsive force between like charges exceeds the surface tension of the droplet (the Rayleigh instability limit). Successive rounds of Rayleigh fission coupled with evaporation are predicted to yield droplets containing a single ion. Evaporation, aided by collisions with gas molecules in the source region is proposed to account for the final desolvation steps until no further solvent can be removed, yielding free ions in the gas phase. This mechanism is known as the charge residue model and is proposed as the universal model for electrospray of large multiply charged species [9]. The counter ions, primarily acetate ions, will be attracted to the positively charged capillary wall. When essentially all the solvent has evaporated the charge will be close to that required for ion evaporation. Multiple protonation will occur by proton transfer from the NH_4^+ ions to the basic residues on the surface of the protein. Prior to this stage the protein ions inside the droplet will have a net charge close to zero since counter ions will serve to neutralise positive and negative charges. For folded globular proteins, the overall charge of the protein, by the time it is recorded in the mass spectrum, has been shown to be close to the number of surface accessible basic sites [10]. The introduction of nanoflow-electrospray has lead to a mechanism in which the protein droplet enters at a much later stage, when the initial droplet size is significantly smaller than for conventional electrospray. This has significant advantages for preserving noncovalent interactions in the gas phase since the energy required to desolvate these ions is significantly reduced [11].

It is well established that proteins in their native state carry fewer charges when compared with denatured states, a phenomenon attributed to the disruption of salt bridges in the unfolded protein. For folded proteins in ammonium acetate buffer at the droplet stage, NH_4^+ ions will be on the surface and the hydrophilic protein molecule will be in the centre of the droplet. However, a consistent feature of the mass spectra of noncovalently assembled particles is that the mass measured for the intact multiprotein complex invariably exceeds that of the mass calculated for the sum of the individual subunits. This excess mass has been attributed to the trapping of water molecules, buffer salts or counter ions within the interstices of the multiprotein complex [12,13]. Evidence for this proposal comes from the displacement of the heterogeneity associated with peak broadening during ligand-binding experiments [14] and the fact that gas-phase association leads to narrower peak widths than are typically observed for solution-based protein interactions. The composition of the small molecules trapped within these macromolecular complexes remains unknown.

The aims of this investigation are twofold: firstly, to disrupt a multiprotein complex through CID and examine the gas-phase dissociation pathways of tetrameric TTR and secondly, to probe the composition of ions formed from multiprotein complexes by investigating fragment ions formed by metastable decay of collisionally activated complex ions. Specifically, we explore the dissociation of the homotetramer TTR (Leu55Pro (L55P) mutant).

2. Experimental

Protein was expressed and purified in our laboratory as described previously [14]. All spectra are acquired on a quadrupole time-of-flight (Q-TOF) 1 instrument (Micromass, Manchester, UK) under conditions optimised for the transmission of noncovalent complexes. Nanoflow-electrospray ionisation (nano-ESI) capillaries are prepared by using a micropipette puller (Flaming/Brown P-97, Sutter Instruments, Novato, CA, USA) and borosilicate glass tubes of 1 mm outer and 0.5 mm inner diameter (Harvard Apparatus, Holliston, MA, USA). These are coated with a thin layer of gold by using an SEM sputter-coater (Polaron, Newhaven, UK) to make them electrically conductive. The pulled end of the capillaries is clipped under a stereomicroscope, resulting in inner tip diameters of between 2 and 5 μm. Two microlitres of the aqueous protein solution were sprayed from these capillaries with the aid of a backing pressure of 0.5 bar.

For tandem-MS, ions in a narrow *m*/*z* window are isolated in the quadrupole analyser and accelerated into an argon-filled linear hexapole collision cell, where they become activated by multiple collisions and eventually dissociate to form a CID product spectrum, recorded in the TOF analyser. The following parameters are typically used for the experiments (positive ion mode): capillary voltage 1.7 kV, cone gas 100 l/h, source temperature 300 K, sample cone 125 V, extractor cone 2 V, and ion energy 2 V. Collision voltage and pressures vary according to the experiment. Typically MS/MS spectra were recorded with a TOF analyser pressure of 4.9×10^{-7} mbar. The spectra recorded under lower collision cell pressure gave rise to a TOF pressure reading of 4.6×10^{-7} mbar. External calibration of the spectra is achieved using solutions of cesium iodide. Data are acquired and processed with MassLynx software (Micromass). All spectra are shown with minimal smoothing and without background subtraction.

3. Results and discussion

The tetramer TTR consists of four identical subunits arranged to form a channel structure, occupied in vivo by the thyroid hormone thyroxin [15]. A typical nano-ESI mass spectrum of L55P TTR from aqueous solution buffered with ammonium acetate at pH 7 is shown in Fig. 1. The predominant signal corresponds to intact homotetramer, labelled Q. The observed charge states extend from 16+ to 13+ with Q^{15+} as the major species. In addition, two peaks at *m*/*z* 1986 and 2316 indicate the presence of monomer (M^{7+} and M^{6+}). Low intensity signal around *m*/*z* 5000 is consistent

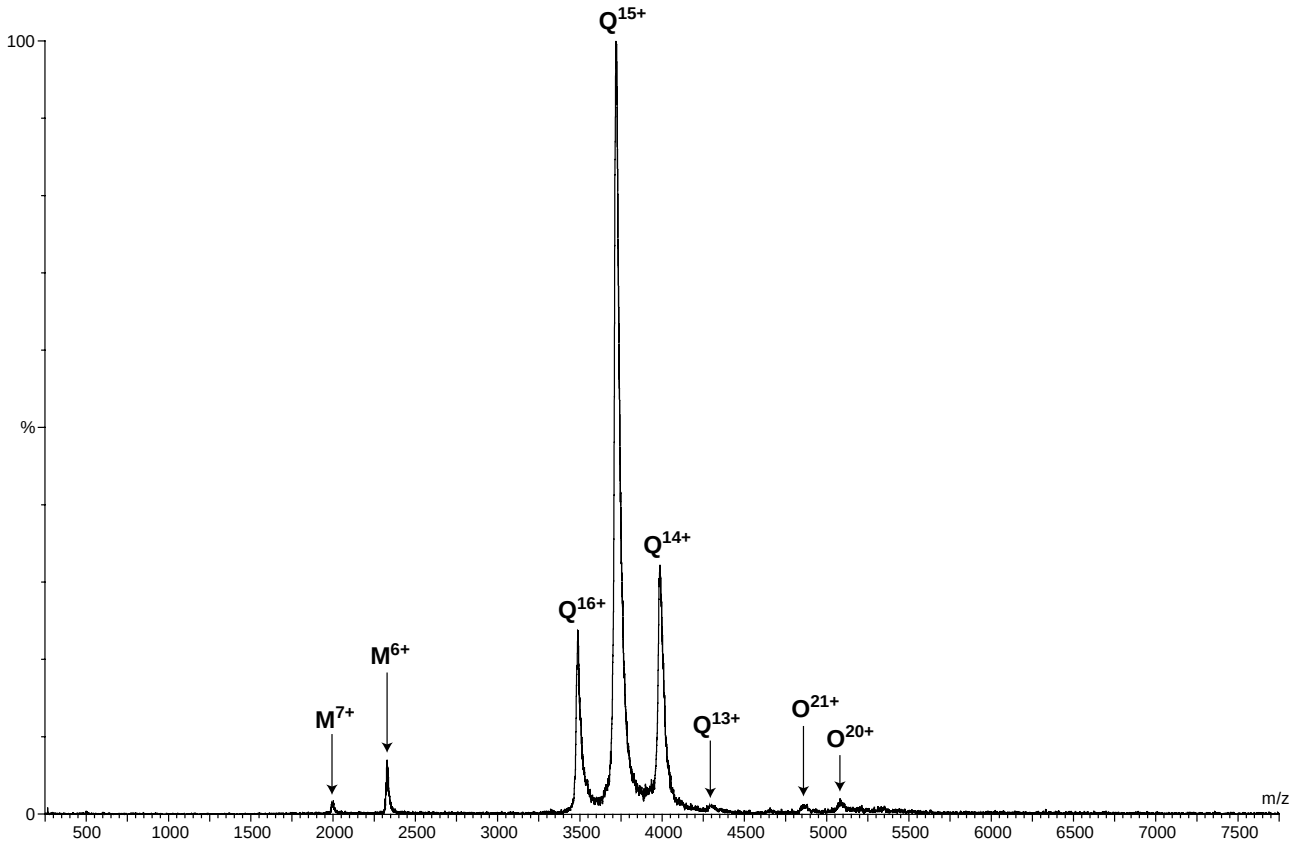

Fig. 1. Nano-ESI spectrum of L55P TTR tetramer (Q, calculated mass 55,506.4 Da) introduced from aqueous solution at pH 7.0 and acquired under non-dissociating conditions. Monomer (M, calculated mass 13,876.6 Da) and octamer (O) are also visible.

with an octameric species (O^{21+} and O^{20+}). These species may originate from solution-phase equilibria; X-ray crystallography also reveals an octameric complex formed from two tetramers [16]. The monomeric form of TTR is implicated in the formation of disease-related amyloid fibrils under physiological conditions [17].

Isolation of the 15+ tetramer charge state and activation in the collision cell gives rise to the spectra shown in Fig. 2. At a collision voltage of 30 V, the Q^{15+} ions pass intact through the collision cell. At 45 V the ions undergo increasingly energetic collisions, and groups of peaks are apparent in the spectrum corresponding to CID products of the tetrameric charge state. Finally, at a collision voltage of 60 V little intact tetramer survives; rather the monomeric and trimeric CID products dominate the spectrum. Around *m*/*z* 1500–2000, highly charged monomers with 7+, 8+ and 9+ charges are observed, accompanied by trimer ions with 8+, 7+ and 6+ charges in the *m*/*z* 5000–7000 range. At least three distinct dissociation pathways are evident for the TTR homotetramer, with a disproportionally high amount of the total charge associated with the monomer.

The trimer and tetramer peaks are consistently broader and the masses higher than would be predicted by straightforward association of monomeric subunits (Table 1). This suggests that the small molecules derived from the solvent are retained in the trimeric structure. Curiously, two small but distinct peaks also appear for the Q^{14+} and Q^{16+} charge states of the tetramer, which imply loss and 'gain' of a positive charge, respectively. While loss of a positive charge from an ion with 15+ charges could occur readily by loss of an ammonium ion, it is difficult to conceive how a 15+ ion could gain further positive charge, e.g., by gas-phase protonation. A more likely explanation for the appearance of the Q^{16+} charge state would, therefore, be loss of an attached negative ion, for example, an acetate ion from the buffer. In spite of the fact that a negative ion attached to a

Table 1
Calculated and observed *m*/*z* values of monomeric (M) and trimeric (T) dissociation products and the tetrameric parent ion (Q) (cf. Fig. 2)

	M^{9+}	M^{8+}	M^{7+}	Q^{16+}	Q^{15+}	Q^{14+}	T^{8+}	T^{7+}	T^{6+}
m/*z* (calculated)	1542.8	1735.6	1983.4	3470.2	3701.4	3965.7	5210.7	5955.0	6947.3
m/*z* (observed)	1543.1	1735.9	1983.6	3479.2	3712.0	3970.5	5219.6	5963.7	6955.3

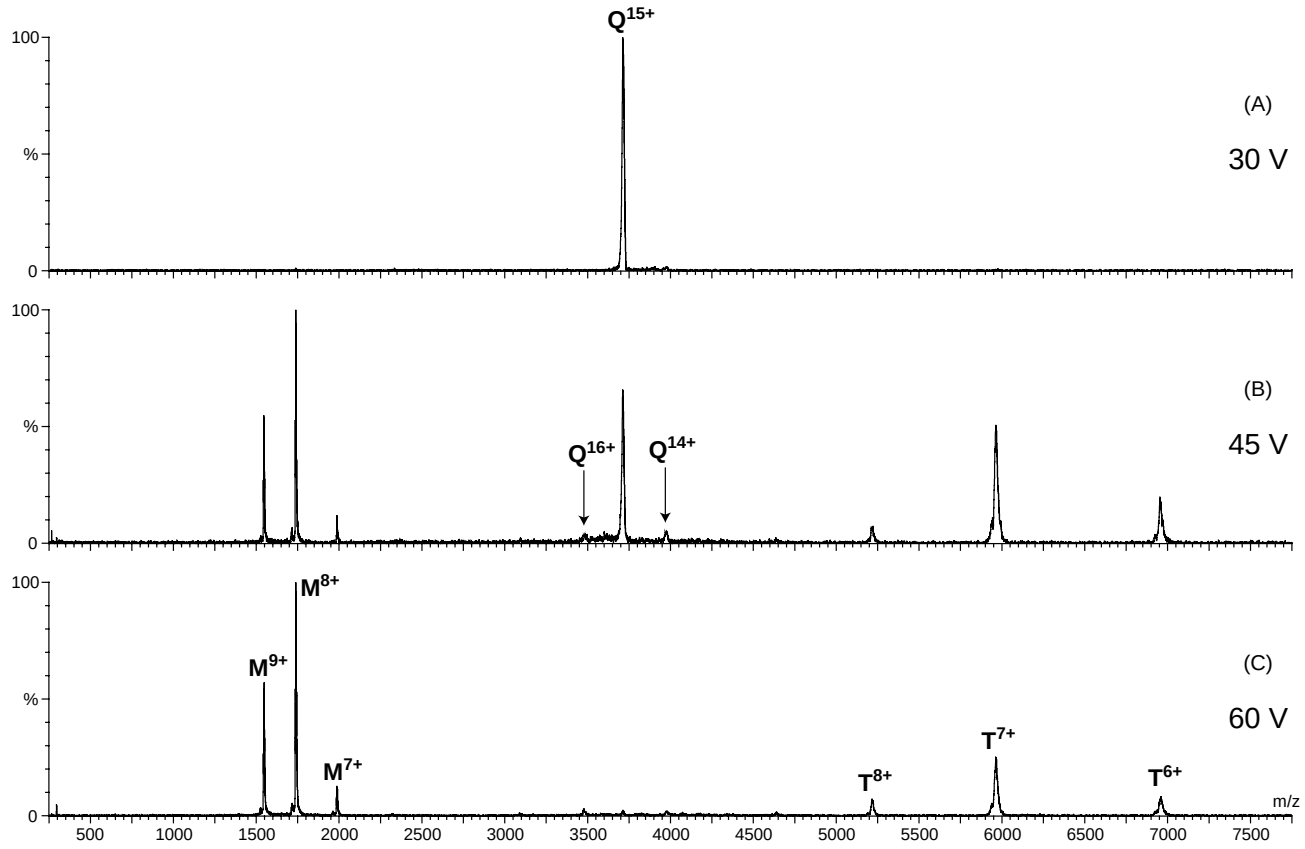

Fig. 2. The effect of increasing collision cell voltage on CID of the isolated Q^{15+} charge state of L55P TTR tetramer. As the collision voltage is increased from 30 to 45 and 60 V (A–C) disruption of the tetramer gives rise to monomeric (M) and trimeric (T) product ions. Small quantities of charge-stripped tetramer ions (Q^{16+} and Q^{14+}) are also produced. Quadrupole analyser pressure 4.2×10^{-5} mbar, TOF analyser pressure 4.9×10^{-7} mbar.

multiply positive-charged complex must experience strong attractive forces, stripping of a negative charge occurs to almost the same extent as the loss of a positive charge. It should be kept in mind, however, that collisions with the comparatively small argon atoms will initially deposit energy in a well-localised area of the much larger molecular ion, such that this process cannot be described by simple equilibrium parameters, such as internal energy [18]. Besides, a counter-ion embedded in the molecular complex or attached to its surface will only experience a fraction of the total charge, and is consequently partly shielded. We have observed apparent 'gain' of positive charge during CID of a number of noncovalent protein complexes. The extent to which this happens correlates with the width of the parent ion peak, indicating that increased heterogeneity of the parent species facilitates the loss of attached ions, both positive and negative.

To investigate the effects of small molecules binding to the molecular ion, the pressure in the collision cell was manipulated, thus affecting the number of collisions which the molecular ions undergo on their passage through the cell. During collisional activation of ions, their initial kinetic energy (which depends on the collision voltage and the charge state of the ion) is converted into internal energy, effectively heating the ions until they decompose [19,20]. Product and parent ions that have survived the CID process but have lost a large proportion of their kinetic energy (only a few eV remaining) will be pulsed into the orthogonal TOF with the correct angle in order to pass the reflectron and reach the detector. At lower collision gas pressure, however, the ions will experience fewer collisions, and activation will happen close to the exit of the collision cell. In spite of the time taken for ions to reach the pusher, on the order of milliseconds, where they are orthogonally

Fig. 3. Decomposition of the isolated Q^{15+} charge state of L55P TTR tetramer during MS/MS analysis. Upper panel: activation of parent ion (Q^{15+}) gives rise to charge-stripped tetramers (Q^{16+} and Q^{14+}), monomers (M^{9+} to M^{7+}, as well as M^{17+} to M^{10+}) and trimers (T^{9+} to T^{6+}). Lower panel: enlarged section of the same spectrum, also showing heptamers (H^{20+} to H^{17+}, see text) and various metastable ions labelled m^*1 to m^*8 (see Table 2). Collision voltage 50–90 V, quadrupole analyser pressure 4.2×10^{-5} mbar, TOF analyser pressure 4.6×10^{-7} mbar. Inset: scheme depicting major pathways of asymmetric dissociation during CID of Q^{15+} tetramer and the underlying signal of O^{30+} octamer.

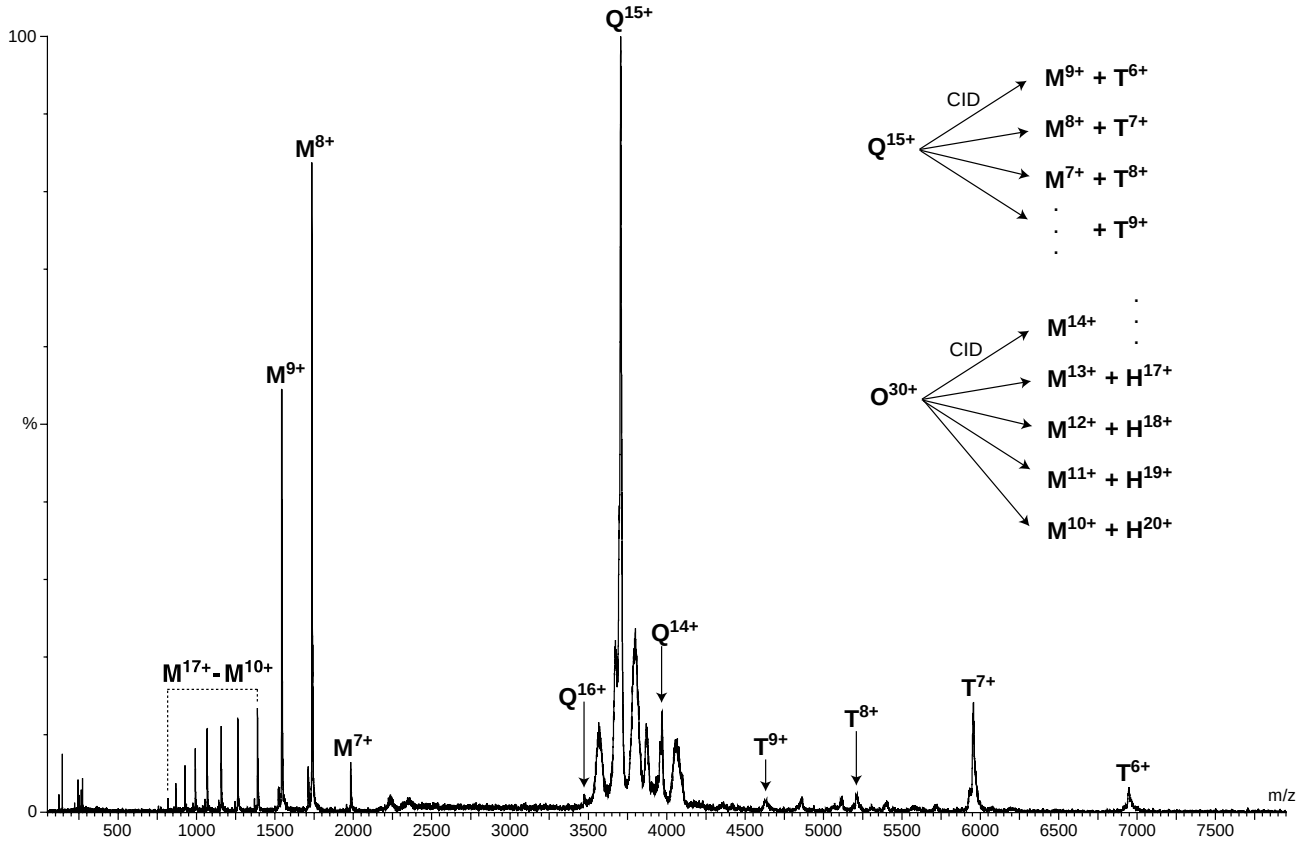
100
%
0
500
1000
1500
2000
2500
3000
3500
4000
4500
5000
5500
6000
6500
7000
7500
m/z
Q15+
M8+
M9+
M17+ - M10+
M7+
Q16+
Q14+
T9+
T8+
T7+
T6+
CID
Q15+
M9+ + T6+
M8+ + T7+
M7+ + T8+
+ T9+
CID
O30+
M14+
M13+ + H17+
M12+ + H18+
M11+ + H19+
M10+ + H20+

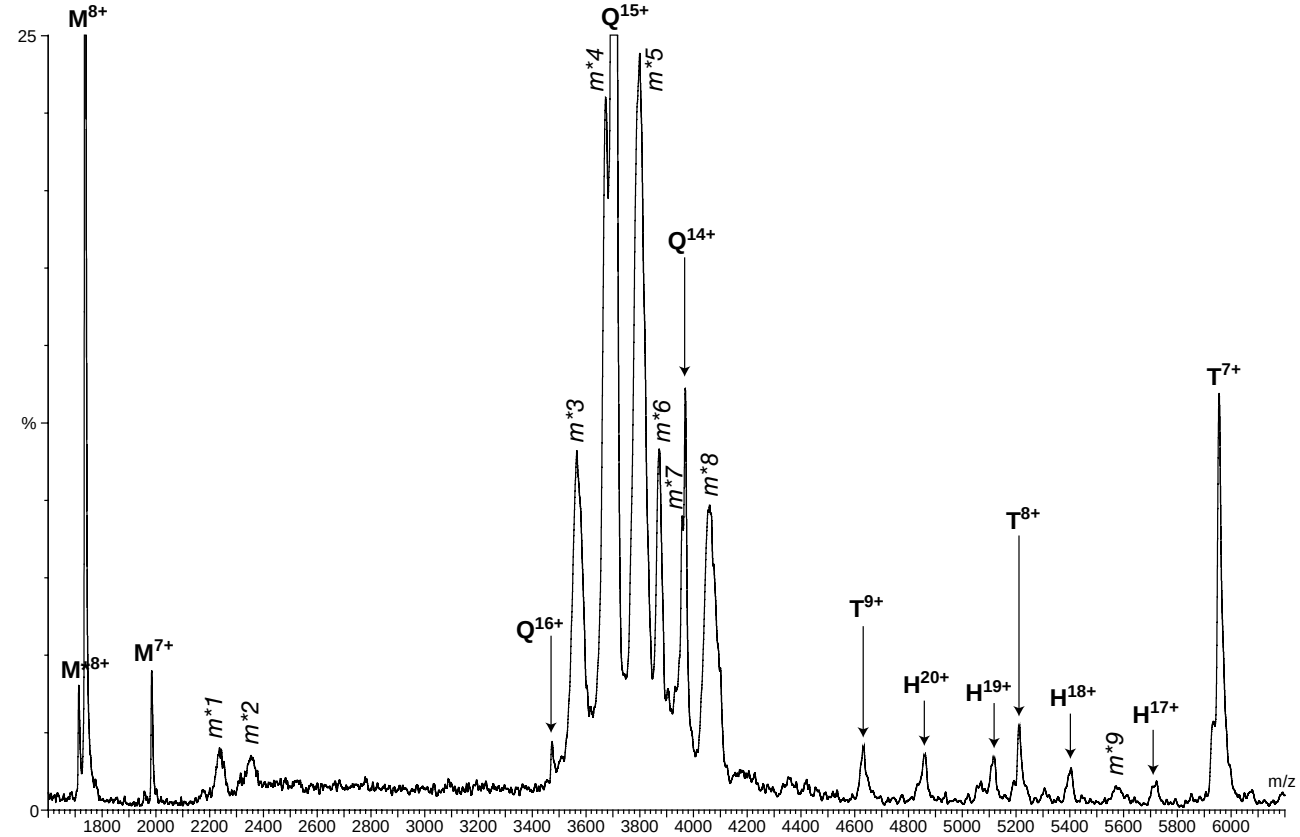
25
%
0
1800
2000
2200
2400
2600
2800
3000
3200
3400
3600
3800
4000
4200
4400
4600
4800
5000
5200
5400
5600
5800
6000
m/z
M8+
M*8+
M7+
m*1
m*2
Q15+
m*4
m*5
Q14+
m*3
m*6
m*7
m*8
Q16+
T9+
H20+
H19+
T8+
H18+
m*9
H17+
T7+

accelerated into the TOF analyser, a proportion will not have decomposed under lower collision gas pressure conditions. When these ions exit the pusher, they decompose in the first field-free TOF drift zone (also termed 'post-pusher decay' ions, PPD [21], by analogy with 'post-source decay' ions in MALDI, PSD). Product ions, which are produced by metastable decay, will have roughly the same velocity as the parent ion but will have lost some kinetic energy according to the mass-to-charge distribution between the products, and thus penetrate the reflectron less deeply. They therefore appear at the detector at a different time than the intact parent ion, and consequently at a different m/z value.

The CID product ion spectrum of the 15+ charge state of the L55P TTR tetramer was also investigated at intermediate collision voltages, but lower collision cell pressure (see Section 2). Fig. 3 shows the familiar pattern of asymmetric dissociation into monomers and trimers. Adjacent to the Q^{15+} parent ion, the tetramers with charge states Q^{16+} and Q^{14+} are also apparent. In addition to ions corresponding to monomeric subunits (7+ to 9+), a group of highly charged monomers is visible with charge states ranging from 17+ to 10+. Close examination of the high m/z region of the spectrum reveals a series of peaks with 20+ to 17+ corresponding in m/z to heptamers. The presence of heptamer indicates that the isolated ion signal labelled as Q^{15+} must also have contained some O^{30+} octamer, at the same m/z ratio.

In addition to well-resolved CID product ions, the spectrum in Fig. 3 also shows a multitude of broad diffuse peaks at around m/z 2200–2400 and 3500–4200. These ions are assigned to ions formed by metastable decay (cf. Table 2). A simple relationship has been deduced to relate the mass-to-charge ratios of the precursor ions with both the focused fragment and the metastable ions (m^*) in orthogonal TOF mass spectrometers [22]:

$$m^* = m_a \left(\frac{1 + (m_b/m_a)r}{1 + r} \right)^2,$$

where r is an instrumental parameter dependent on the relative electrical potentials and path length of the reflectron-TOF mass spectrometer (for the Q-TOF it was determined as $r = 0.606$), and m_a and m_b are parent and product ion mass-to-charge ratios, respectively. Substitution of the precursor and product ions into the above formula reveals that the metastable products m^*1 and m^*2 were formed from the decomposition of TTR tetramer Q^{15+} to the monomers M^{9+} and M^{8+}, respectively. The two major dissociation pathways give rise to these two monomer charge states and also to the two dominant metastable ions at m/z ~2300.

The group of peaks around the Q^{15+} tetramer, labelled m^*3 to m^*8, is assigned to species which were formed by metastable loss of positive or negative charges from an intact tetramer (Table 2). According to this interpretation, the broad peaks m^*3, m^*5 and m^*8 correspond to the loss of a singly charged negative ion from Q^{15+}, Q^{14+} and Q^{13+}, respectively, giving rise to an apparent increase in charge as discussed above. The concomitant small change in mass has been neglected for the calculations as it does not contribute significantly to the total mass. The somewhat narrower metastable peaks m^*4 and m^*7 indicate loss of a single positive charge (most likely, an ammonium ion) from the Q^{16+} and Q^{15+} ions, respectively. The metastable peak at m^*6 is believed to arise from the transition $Q^{13+} \rightarrow Q^{15+}$ and involves either the gain of two positive charges or loss of two negative charges simultaneously. Since simultaneous gain of two positive charges is unlikely the results appear to be consistent with loss of a doubly charged anion, such as phosphate or sulphate ions, present as impurities in the protein solution.

The width of metastable ions is attributed to the spread of kinetic energies in the resulting fragment ions. Losses of small positively charged ions yield narrow metastable peaks (m^*4 and m^*7) implying that most of the energy is carried by the lighter fragment leading to a narrow peak. Consequently, the broader peaks observed for an increase in positive charge (or decrease in negative charge) could arise from more than one pathway, presumably with a wide mass range, such as protonation from NH_4^+ or H_3O^+, or loss of acetate ions, HSO_4^- or HPO_4^-. Interestingly, the most intense metastable ions originate from

Table 2
Calculated and measured masses of parent, product and associated metastable ions (cf. Figs. 3 and 4)

	m^* (metastable)			m_a (parent)			m_b (product)	
	m/z (calculated)	m/z (observed)		m/z (calculated)	m/z (observed)		m/z (calculated)	m/z (observed)
m^*1	2251.6	2236.8	Q^{15+}	3701.4	3706.0	M^{9+}	1542.8	1543.8
m^*2	2366.5	2353.4	Q^{15+}	3701.4	3706.0	M^{8+}	1735.6	1736.3
m^*3	3529.0	3565.7	Q^{15+}	3701.4	3706.0	Q^{16+}	3470.2	3473.5
m^*4	3646.9	3672.7	Q^{16+}	3470.2	3473.5	Q^{15+}	3701.4	3706.0
m^*5	3768.7	3799.8	Q^{14+}	3965.7	3969.4	Q^{15+}	3701.4	3706.0
m^*6	3851.9	3872.2	Q^{13+}	4270.7	n/o	Q^{15+}	3701.4	3706.0
m^*7	3903.5	3957.8	Q^{15+}	3701.4	3706.0	Q^{14+}	3965.7	3969.4
m^*8	4043.6	4060.5	Q^{13+}	4270.7	n/o	Q^{14+}	3965.7	3969.4

n/o indicates that the parent ion is not observed but is inferred by observation of the corresponding metastable and product ions.

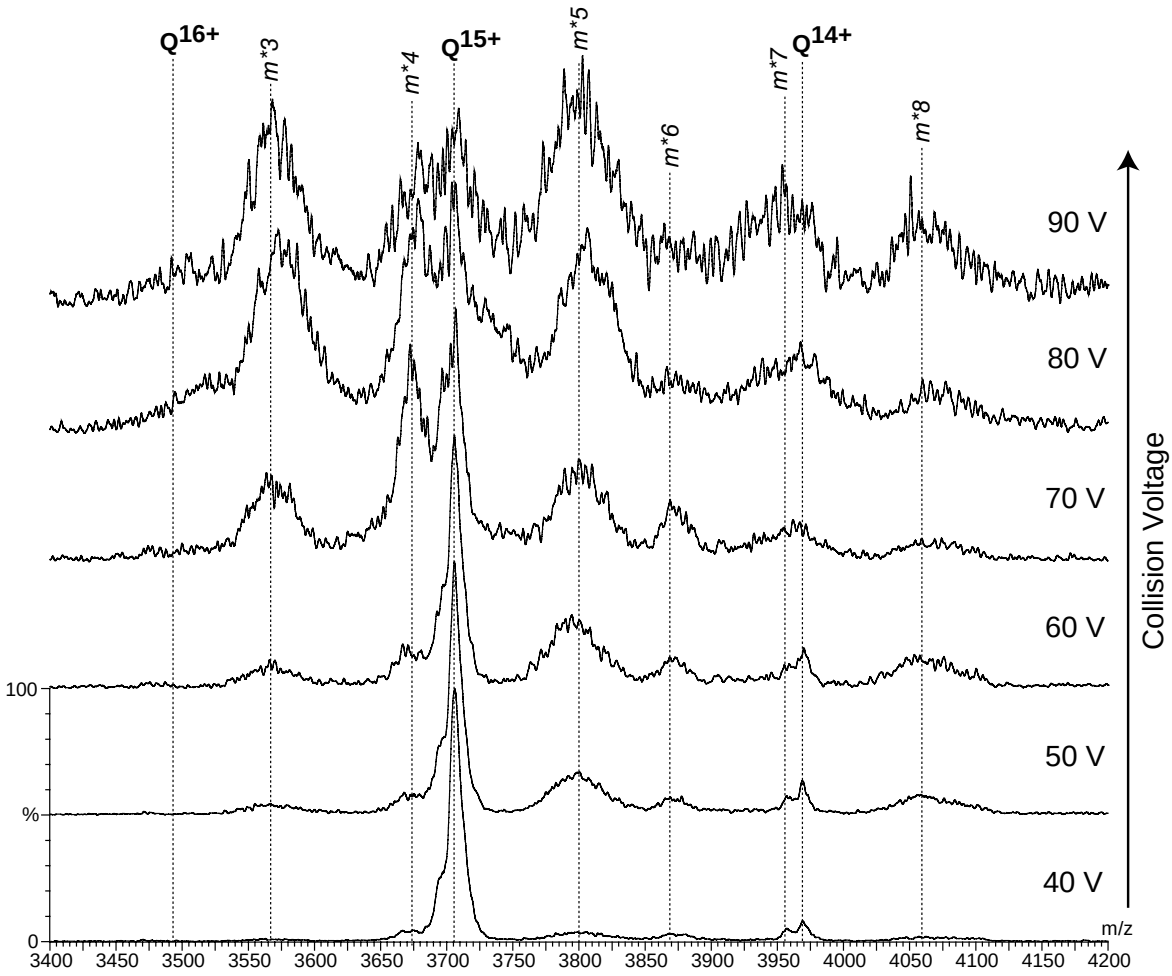

Fig. 4. The effect of increasing collision voltage on the appearance of metastable peaks formed by loss of ions derived from the buffer solution (same experimental conditions as in Fig. 3).

parent ions that have already undergone charge stripping indicating that they are sufficiently activated in the collision cell to undergo further losses in a slow, metastable process.

The effects of increasingly energetic collisions on the appearance of these metastable ions was investigated by a stepwise increment of the collision voltage. The results shown in Fig. 4 indicate that at the lowest energy essentially only the isolated tetramer Q^{15+} is present with a small amount of Q^{14+} charge state formed by loss of a positive charge. As the energy is increased this transition to form the Q^{14+} charge state becomes more prominent and the metastable ion m^*5 for formation of $Q^{14+} \rightarrow Q^{15+}$ via loss of negative charge becomes apparent. Significantly, the m^*3 signal for the transition $Q^{15+} \rightarrow Q^{16+}$ is only observed at higher collision cell voltages, indicating that the stripping of negative ions from the more highly charged tetramers requires more energy than the transition ($Q^{14+} \rightarrow Q^{15+}$). At a collision cell voltage of 90 V, the parent ion signal Q^{15+} is of comparable low intensity to the metastable ions m^*3 and m^*5. From this series of experiments, it can be concluded that dissociation of the tetramer occurs concomitantly with loss of ions derived from the buffer and implies that these ions are an integral part of multiprotein complexes that perhaps contribute to their stability in the gas phase.

4. Conclusion

We have shown that during CID of tetrameric TTR ions, both trimer and monomer products are formed. As the collision energy is increased, the intensity of the tetramer decreases until trimer and monomer peaks dominate the spectra. The fact that the protein variant (L55P TTR) is known to be partially folded under the solution conditions employed here suggests that this structure may be capable of trapping an increased distribution of buffer molecules. During CID these ions are released giving rise to multiple protonation/deprotonation events, from trapped NH_4^+ and acetate ions, and hence a broader charge state distribution for the parent complex ions. The lower surface area of the

monomer is less likely to trap adducted ions than the trimer or tetramer species consistent with the increased masses observed for the latter species suggesting that they retain heterogeneity of small molecule binding, presumably in the interfacial regions of the protein complex.

Further evidence for the dissociation pathways comes from the metastable ions observed for the decomposition of the tetramer to both monomeric and trimeric products. The observation of metastable ions for changes in charge state of the tetrameric ion, however, was unexpected but serves to demonstrate the presence of buffer molecules in the composition of these gas-phase species. For the 15+ charge state of the TTR tetramer a peak width of m/z 28 was recorded. The presence of a single ammonium or acetate ion added to the theoretical isotope distribution of the molecular ion and taking into account the resolution of the instrument would contribute to peak broadening with m/z 1.2 and 2.8, respectively. The observed peak widths suggest, therefore, that a convolution of small molecules and ions are adducted to the protein complex.

How does this fit in with current views of the electrospray mechanism? From the evidence presented here, it is apparent that not all ions from the buffer solution are lost to the capillary wall or during the final desolvation stages. Rather a heterogeneous distribution of solvent-derived ions, both positively and negatively charged, appear to be present in these gas-phase multiprotein complex ions. This heterogeneous distribution of small ions that coexist within these gas-phase macromolecular structures may contribute to their stability after their transfer into the gas phase.

Acknowledgements

We thank Keith Jennings (Warwick University), Bob Bateman (Micromass, Manchester, UK) and Igor Chernushevich (Sciex, Concord, Ont., Canada) for helpful discussions, and the Royal Society and Wellcome Trust for funding.

References

[1] A.A. Rostom, C.V. Robinson, Curr. Opin. Struct. Biol. 9 (1999) 135.
[2] J. Loo, Int. J. Mass Spectrom. 200 (2000) 175.
[3] F. Sobott, C.V. Robinson, Curr. Opin. Struct. Biol. 12 (2002) 729.
[4] B.L. Schwartz, D.C. Gale, R.D. Smith, J. Mass Spectrom. 30 (1995) 1095.
[5] J. Jurchen, E. Williams, J. Am. Chem. Soc. 125 (2003) 2817.
[6] C. Versluis, A. Van der Staaij, E. Stokvis, A.J.R. Heck, B.d. Craene, J. Am. Soc. Mass Spectrom. 12 (2001) 329.
[7] M. Fandrich, M.A. Tito, M.R. Leroux, A.A. Rostom, F.U. Hartl, C.M. Dobson, C.V. Robinson, Proc. Natl. Acad. Sci. U.S.A. 97 (2000) 14151.
[8] F. Sobott, H. Hernandez, M.G. McCammon, M.A. Tito, C.V. Robinson, Anal. Chem. 74 (2002) 1402.
[9] J.F. de la Mora, G.J. Van Berkel, C.G. Enke, R.B. Cole, M. Martinez-Sanchez, J.B. Fenn, J. Mass Spectrom. 35 (2000) 939.
[10] P. Kebarle, M. Peschke, Anal. Chim. Acta 406 (2000) 11.
[11] E.W. Chung, D. Henriques, D. Renzoni, J.E. Ladbury, C.V. Robinson, Protein Sci. 8 (1999) 1962.
[12] J.A. Loo, Mass Spectrom. Rev. 16 (1997) 1.
[13] E.J. Nettleton, M. Sunde, V. Lai, J.W. Kelly, C.M. Dobson, C.V. Robinson, J. Mol. Biol. 281 (1998) 553.
[14] M.G. McCammon, D.J. Scott, C.A. Keetch, L.H. Greene, H.E. Purkey, H.M. Petrassi, J.W. Kelly, C.V. Robinson, Structure 10 (2002) 851.
[15] C.C.F. Blake, M.J. Geisow, S.J. Oatley, B. Rerat, C. Rerat, J. Mol. Biol. 121 (1978) 339.
[16] M. Sebastiao, M. Saraiva, A. Damas, J. Biol. Chem. 273 (1998) 24715.
[17] H.A. Lashuel, Z.H. Lai, J.W. Kelly, Biochemistry 37 (1998) 17851.
[18] A.K. Shukla, J.H. Futrell, J. Mass Spectrom. 35 (2000) 1069.
[19] M.R. Mauk, A.G. Mauk, Y.-L. Chen, D.J. Douglas, J. Am. Soc. Mass Spectrom. 13 (2002) 59.
[20] V. Nesatyy, J. Laskin, Int. J. Mass Spectrom. 221 (2002) 245.
[21] C. Versluis, A. Van der Staaij, E. Stokvis, A.J.R. Heck, B.D. Craene, J. Am. Soc. Mass Spectrom. 12 (2001) 329.
[22] D.J. Harvey, A.P. Hunter, R.H. Bateman, J. Brown, G. Critchley, Int. J. Mass Spectrom. 188 (1999) 131.